Southern Horizons in Time-Domain Astronomy
Proceedings IAU Symposium No. 339, 2019
E. Griffin, ed.

doi:10.1017/S1743921318002867

Phase-resolved Spectroscopy and Photometry of the Eclipsing Polar UZ Fornacis†

Z. N. Khangale[1,2], S. B. Potter[1] and P. A. Woudt[2]

[1]South African Astronomical Observatory, Cape Town, South Africa
email: khangalezn@saao.ac.za

[2]Department of Astronomy, University of Cape Town, Cape Town, South Africa

Abstract. The blue continuum of the eclipsing polar UZ For is dominated by single- or double-peaked emission from He II, He I and the Balmer lines. The red spectrum shows weak emission from the Na I doublet at λ8183 and 8194 Å and strong emission from the Ca II lines at λ8498 and 8542 Å. Doppler tomography of the strongest emission features reveals the presence of emission from the irradiated face of the secondary star, the threading region, and the ballistic and magnetically confined accretion stream. We have obtained 28 new eclipse times of UZ For during 2011–2016 as part of our eclipse timing follow-up programme to test the two-planet model proposed to explain variations in the eclipse times of UZ For.

Keywords. Accretion, accretion disks – techniques: photometric, spectroscopic – stars: individual: UZ For – cataclysmic variables-planetary systems

1. Introduction

UZ Fornacis is an eclipsing polar, discovered by EXOSAT to be an X-ray source, EXO 033319-2554.2 (Giommi *et al.* 1987). It has an orbital period of ∼126.5 min and has been studied extensively at a wide range of wavelengths including optical and X-ray, and by polarimetry. Eclipses of UZ For have been monitored frequently with many different facilities, and a baseline of ∼34 years has been established. Analysis of the mid-eclipse times of the binary by Potter *et al.* (2011), aimed at detecting variations in the orbital period, revealed a departure from linear and quadratic trends with an amplitude of ∼60 sec. These departures suggests the presence of two cyclic variations, of 16(3) and 5.25(25) years. The two favoured mechanisms that could cause the periodicities are either two giant extrasolar planets as companions to the binary, or a magnetic-cycle mechanism of the secondary star.

2. Observations

We obtained 28 new high time-resolution, high S/N ratio eclipses of UZ For between 2011–2016 with the SAAO 1.9-m telescope, using the Sutherland High-speed Optical Camera (SHOC; Coppejans *et al.* 2013) and the HIgh-speed Photo-POlarimeter (HiPPO; Potter *et al.* 2010). Medium-resolution, long-slit spectra (width 1″.5) were obtained in January 2013 with the Southern African Large Telescope (SALT; Buckley *et al.* 2006) using the Robert Stobie Spectrograph (Burgh *et al.* 2003). A total of 23 blue and 14 red medium-resolution spectra with 360-sec exposures and a wavelength coverage of ∼4050–5100Å and ∼7550–8650Å was obtained. The spectroscopic and photometric data

† For the full poster, see http://dx.doi.org/10.1017/S1743921318002867

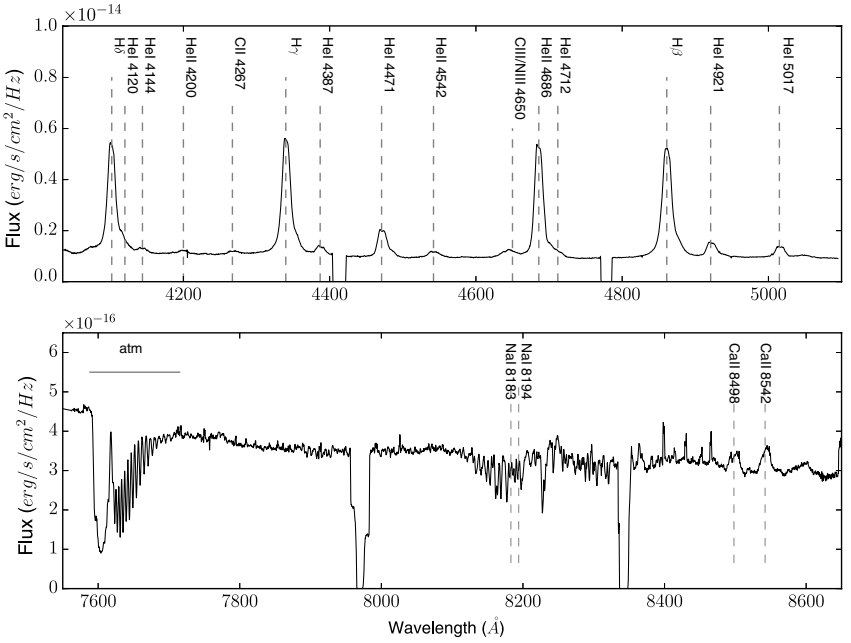

Figure 1. The average wavelength-calibrated blue (top) and red (bottom) spectra of UZ For obtained with SALT. Prominent emission and/or absorption features are labelled.

were reduced using PYSALT and IRAF routines. The averaged blue and red spectra of UZ For are shown in Fig. 1.

3. Results

3.1. *Variations in eclipse times*

The 28 new mid-eclipse times were added to the 42 mid-eclipse times listed by Potter *et al.* (2011). We used least-squares fitting to determine the fitting parameters. The updated (O–C) diagram (Fig. 2) is consistent with earlier conclusions from Potter *et al.* (2011) regarding the presence of two cyclic variations of 5.25(25) and 16(3) years. The refined two-cyclic variations are 5.17(2) and 14.76(3) years, respectively. In our case the outer planet is required to have an eccentricity of 0.4–0.5, but it is difficult to conceive of stable orbits that have such high eccentricity. The new eclipse times agree with the predictions, and the two-cyclic variations are well within the uncertainty of the solution presented by Potter *et al.* (2011).

3.2. *Spectral Analysis*

The top panel of Figure 1 shows the averaged blue spectrum dominated by single- and/or double-peaked emission from the Balmer lines, He II and He I lines. He II λ 4686 Å and the Balmer lines dominate the continuum, but the former is the strongest feature. The Balmer decrement is steep in the case of UZ For. The other lines, the Bowen blend (C III/N III at λ 4650 Å) and C II λ 4267 Å all appear in weak emission. The red spectrum (bottom panel of Fig. 1) shows weak absorption from Na I at λ 8183 and 8194 Å, and also strong emission from the Ca II lines at λ 8498 and 8542 Å. We used the strongest features, i.e. He II λ 4686 Å and the Balmer lines, from both blue spectra, to compute Doppler maps of emission lines for further investigation.

https://doi.org/10.1017/S1743921318002867 Published online by Cambridge University Press

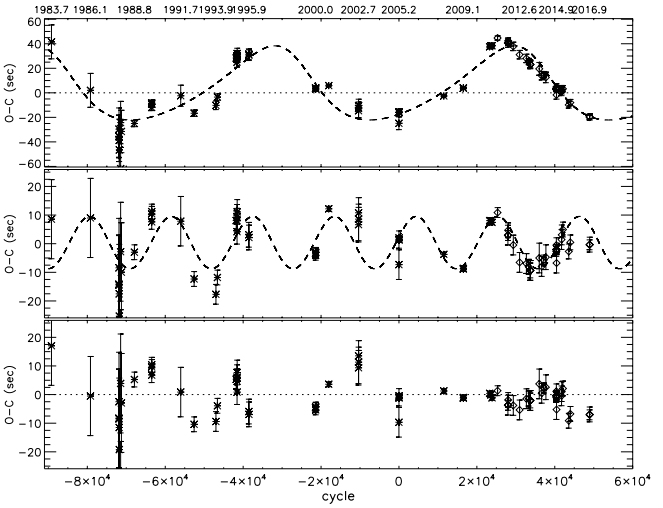

Figure 2. The O–C diagram of UZ For after successive subtraction of the three terms constructed using the fitting parameters, obtained using all the eclipse times of UZ For. Our new data are included in the fitting.

3.3. *Flux Modulation; Doppler Mapping*

We performed Doppler tomography of the strongest emission lines using the inside-out technique developed by Kotze *et al.* (2015), and over-plotted a model with the following properties: $M_1 = 0.3\ M_\odot$, mass ratio $q = \frac{M_2}{M_1} = 0.25$, and inclination $i = 81°$. The observed and reconstructed trailed spectra (Fig. 3, bottom panels) show three distinct components: (1) a relatively narrow component with low amplitude that is associated with the irradiated face of the secondary, (ii) a broad emission component with a high-velocity amplitude, and (iii) a broad feature which is visible throughout the orbital phases. The latter two features are produced in various parts of the accretion flow. Both the standard and the inside-out (averaged) Doppler maps (Fig. 3, top and middle panels) show emission dominated by the threading region, the irradiated face of secondary star, and emission from the ballistic and magnetically confined accretion stream. The modulation amplitude maps (Fig. 3, centre, top and middle) show that the ballistic and the magnetically-confined stream are the most flux-modulated components. The flux of the secondary star is also shown to modulate. The poster (URL on p. 314) discusses the phase of the maximum flux maps and gives more details about the Doppler maps.

3.4. *Discussion*

The cyclical variations in UZ For are consistent with the presence of two planets in elliptical orbits around the binary, or some form of Applegate's mechanism (Applegate 1992). Similar variations in the eclipse times of (for example) NN Ser (Beuermann *et al.* 2010) and HU Aqr (Qian *et al.* 2011) have also been attributed to the presence of one or more companions in orbit around them, or to magnetic activities of the secondary star. The inside-out technique exposes better the low-velocity emission details, which are too compact in standard tomograms. Most of the features discussed above are more pronounced in the inside-out Doppler maps.

References

Applegate, J. H. 1992, *ApJ*, 385, 621

https://doi.org/10.1017/S1743921318002867 Published online by Cambridge University Press

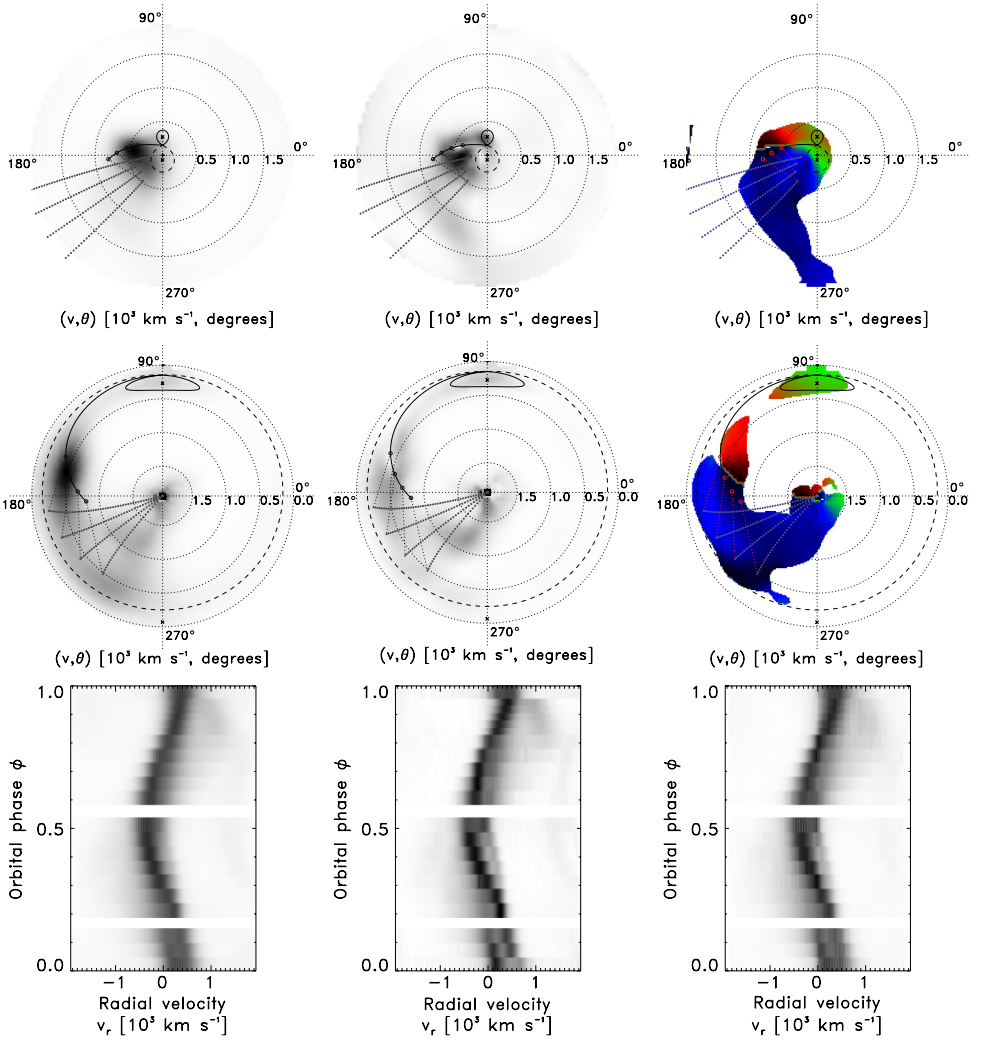

Figure 3. Standard (top row) and inside-out (middle row) Doppler tomography; averaged map (left), modulation amplitude (centere) and phase of maximum flux (right) maps. Bottom panels: observed (centre) and reconstructed trailed (left and right) spectra of He II 4686 Å.

Beuermann, K., *et al.* 2010, *A&A*, 521, L60
Buckley, D. A. H., Burgh, E. B., Cottrell, P. L., Nordsieck, K. H., O'Donoghue, D., & Williams, T. B. 2006, in: I. S. McLean & M. Iye (eds.), *Proc. SPIE*, 6269
Burgh, E. B., Nordsieck, K. H., Kobulnicky, H. A., Williams, T. B., O'Donoghue, D., Smith, M. P., & Percival, J. W. 2003, in: M. Iye & A. F. M. Moorwood (eds.), *Instrument Design and Performance for Optical/Infrared Ground-based Telescopes (Proc. SPIE)*, 4841, 1463
Coppejans, R., *et al.* 2013, *PASP*, 125, 976
Giommi, P., Angelini, L., Osborne, J., Stella, L., Tagliaferri, G., Beuermann, K., & Thomas, H.-C. 1987, *IAU Circ.*, 4486, 1
Kotze, E. J., Potter, S. B., & McBride, V. A. 2015, *A&A*, 579, A77
Potter, S. B., *et al.* 2010, *MNRAS*, 402, 1161
Potter, S. B., *et al.* 2011, *MNRAS*, 416, 2202
Qian, S.-B., *et al.* 2011, *MNRAS*, 414, L16

https://doi.org/10.1017/S1743921318002867 Published online by Cambridge University Press